Substrate Topography Induces a Crossover from 2D to 3D Behavior in Fibroblast Migration

Marion Ghibaudo, Léa Trichet, Jimmy Le Digabel, Alain Richert, Pascal Hersen, and Benoît Ladoux*
Laboratoire Matière et Systèmes Complexes (MSC), Université Paris Diderot and Centre National de la Recherche Scientifique, Unite Mixte de Recherche 7057, Paris, France

ABSTRACT In a three-dimensional environment, cells migrate through complex topographical features. Using microstructured substrates, we investigate the role of substrate topography in cell adhesion and migration. To do so, fibroblasts are plated on chemically identical substrates composed of microfabricated pillars. When the dimensions of the pillars (i.e., the diameter, length, and spacing) are varied, migrating cells encounter alternating flat and rough surfaces that depend on the spacing between the pillars. Consequently, we show that substrate topography affects cell shape and migration by modifying cell-to-substrate interactions. Cells on micropillar substrates exhibit more elongated and branched shapes with fewer actin stress fibers compared with cells on flat surfaces. By analyzing the migration paths in various environments, we observe different mechanisms of cell migration, including a persistent type of migration, that depend on the organization of the topographical features. These responses can be attributed to a spatial reorganization of the actin cytoskeleton due to physical constraints and a preferential formation of focal adhesions on the micropillars, with an increased lifetime compared to that observed on flat surfaces. By changing myosin II activity, we show that actomyosin contractility is essential in the cellular response to micron-scale topographic signals. Finally, the analysis of cell movements at the frontier between flat and micropillar substrates shows that cell transmigration through the micropillar substrates depends on the spacing between the pillars.

INTRODUCTION

Many cellular processes, such as growth, differentiation, motility, and tumor metastasis, involve adhesion of living cells to external surfaces (1,2). Various factors, such as different chemoattractants, temperature, rigidity, and topography of the extracellular matrix (ECM), can modify cell migration by changing signal transduction pathways that affect cytoskeleton organization. The mechanisms and regulation of cell migration have been studied extensively in two-dimensional (2D) cell culture models. However, discrepancies between the behavior of cells in culture and in vivo have led growing numbers of research groups to switch to three-dimensional (3D) models, which better represent the microenvironment of living cells and tissues (3).

3D matrices include complex chemical, physical, and topographical components, and many cellular structures, such as stress fibers or focal adhesions (FAs), can appear less obvious than familiar structures in flattened cells on 2D substrates (4). However, the complexity of in vivo 3D environments makes it difficult to study the influence of external physical factors on cell migration. Remodeling the 3D ECM can affect simultaneously the physical and biochemical characteristics of the matrix. For instance, changing the porosity of the environment can modify the stiffness and the local topography as well as the ligand density. Moreover, when considering tissue-engineering 3D scaffolds, the combined biochemical and physical properties of the ECM are also important regulators in the attachment and migration of cells (5).

Microfabricated substrates with well-defined parameters can be used to study and uncouple the influence of the different physical components on cell adhesion and migration. Controlling the mechanical properties of the surrounding environment is an important issue because accumulating evidence shows that they affect many cellular functions (6,7). For instance, substrate stiffness can modify cell adhesion and migration (8–10), as well as external tensions (11). Along the same line, many studies have focused on micro- and nanotechnologies to develop well-defined environments with the goal of understanding cell responses to guidance signals induced by substrate topography. It has been shown that these topographical cues, such as lines (12,13), ridges (14), columns (15,16), and pits (17), can guide cell adhesion and migration.

The development of numerous strategies to analyze the cellular response to substrate topography has provided new insights into the interactions of cells with their microenvironments, especially in terms of cell shape, cytoskeleton organization, and FA remodeling (15,17). In particular, cells on substrates composed of pillars or pits exhibit spindle shape and pseudopodial protrusions, more akin to the in vivo situation. It has been suggested that these pseudopods can insert into gaps in 3D matrices and serve as anchoring points to pull the cell body (18). The ability of cells to penetrate in 3D environments, as well as the success of tissue-engineering

Submitted October 28, 2008, and accepted for publication April 15, 2009.

*Correspondence: benoit.ladoux@univ-paris-diderot.fr

Editor: Marileen Dogterom.

0006-3495/09/07/0357/12 $2.00

doi: 10.1016/j.bpj.2009.04.024

scaffolds, requires multiple balances between integrin activity, cell contractility, proteolysis, and matrix rearrangements, and depends on the matrix pore size (19,20). However, our knowledge about how cells detect the topography of their enviromments, move over long timescales, and respond in terms of cytoskeleton reorganization and formation of adhesive contacts in a 3D environment is still limited. Systematic studies of cell migration in well-defined topographical substrates provide a useful tool to mimic some of the cellular processes involved in a 3D matrix.

In this study we employed photolithographic techniques to generate physical features on undeformable elastomeric substrates that bear some similarity to the structure of 3D fibrous matrices. We used regular arrays of microsized pillars with different geometries to determine the responses of fibroblasts in topography sensing. Observations of cell adhesion and migration, subsequent morphological and cytoskeletal observations, and cell motility measurements were used to determine cellular interactions with these various microenvironments. We observed that cell migration was governed by diffusion dynamics that depended on the geometrical parameters of the substrate. Analysis of the mean-square displacement (MSD) was used to study the influence of substrate topography on cell migration. Our results also suggest that the organization of the actin cytoskeleton and FAs give fibroblastic cells the capacity to orient and migrate through micron-sized patterns. In particular, we observed that the lifetime of FAs increased on micropillar substrates, and that myosin II and cell contractility play an important role in the migration process. Finally, by studying cellular transmigration at the frontier between a 2D surface and a micropillar substrate, we found that the topography could guide the directionality of cell migration depending on the micropillar spacing. Taken together, these results allow us to propose a mechanism of cell migration in micropillar substrates based on the formation of cellular protrusions that are stabilized by the presence of micropillars. Since the patterned surface aims to mimic a basic structural element of a 3D environment, this study may provide information on the mechanisms that govern 3D migration, as well as relevant pore sizes for future tissue-engineering scaffolds that encourage cell migration and penetration.

MATERIALS AND METHODS

Cell cultures and transfections

3T3 cells were maintained at 37°C in a humidified atmosphere of 5% CO_2 and 95% air in Dulbecco's modified Eagle medium (DMEM) containing 10% bovine calf serum, 100 U/mL penicillin, 100 μg/mL streptomycin, and 100 μg/mL glutamine. 3T3 cells were transfected with the use of Nanofectin reagent (PAA, Pasching, Austria) in a 35 mm petri dish, using enhanced green fluorescent protein (EGFP)-vinculin plasmid (kindly provided by Dr. M. Coppey, Institut Jacques Monod, Paris, France) according to the PAA protocol. Transfected cells were observed for 24–48 h after transfection. Blebbistatin was added to the medium at a 75 μM concentration using a 03 FCG 089 filter (Melles Griot, Voisins le Bretonneux, France) on the light path. We registered the cells' behavior every 5 min at different positions.

Fabrication and characterization of microstructured polydimethylsiloxane substrates

Polydimethylsiloxane (PDMS; Sylgard 184, Dow Corning, Midland, MI) micropillar arrays were prepared according to du Roure et al. (21). Briefly, PDMS was poured over a silicium wafer, cured at 65°C for 15 h $\pm$ 2 h, and peeled off the wafer under dry conditions. PDMS substrates were immersed for 1 h with fibronectin (20 μg/mL; Sigma-Aldrich, Saint-Quentin Fallavier, France) in phosphate-buffered saline (PBS) (22). We used a consistent cure time of 15 h $\pm$ 2 h at 65°C corresponding to a Young's modulus of 2 MPa $\pm$ 0.1 MPa, and used scanning electron microscopy (SEM) to measure the dimensions of the pillars as previously described (21).

Time-lapse video microscopy

We acquired time-lapse images of cells on pillars on an Olympus BX51 upright and an Olympus IX71 inverted microscope (Olympus, Rungis, France), both of which were equipped with a on-stage heater to maintain the temperature at 37°C (LIS, Basel, Switzerland). To prevent gas exchange and water evaporation, the culture medium was covered with a thin layer of mineral oil after the addition up to 45 mM HEPES into the solution to maintain a constant pH. Images were acquired with Photometrics Coolsnap ES (inverted microscope) and HQ^2 (upright microscope) cameras (Roper Scientific, Evry, France) using Metamorph software (Universal Imaging Corporation, Downingtown, PA).

For the 3T3 trajectory experiments, time-lapse sequences were acquired during 24 h using a frame delay of 5 min on the inverted microscope. Images were taken using an Olympus 20$\times$ air objective (NA 0.40). We acquired six to eight different positions using a motorized stage (Marzhauser, Wetzlar, Germany).

Quantitative analysis of individual cell motility

To quantify cell migration, we analyzed the time-lapse images with ImageJ plugins. To follow individual cells, we tracked their center of mass. First, we used a fast Fourier transform bandpass filter to eliminate the pillars from the pictures. We chose the lower bound to be similar to the pillar spacing/size, and the upper bound larger than the cell size. This procedure allowed us to eliminate the pillars from the acquired images. To enhance the contrast of the image, we then subtracted the image background and used the Particle tracker plugin for cell tracking (23). Briefly, the procedure is based on determining the fit of the cells within the image with a disk shape by considering the brighter pixels in the images (over a defined threshold). The positions of the disk center can then be recorded.

By knowing all the positions as a function of time, we determined the cell speed and the MSD, $\langle d^2 \rangle$. For each substrate, MSD curves were fitted over time (~550 min) by averaging 10 trajectories, corresponding to cell tracking for at least 1000 min.

The linear speed, V, was calculated by simply dividing the integrated travel distance by the total time of the trajectory T:

$$V = \sum \frac{\sqrt{(x_i - x_{i-1})^2 + (y_i - y_{i-1})^2}}{T}, \tag{1}$$

where x_i and y_i are coordinates at frame i.

The MSD was determined by the following equation:

$$\begin{aligned} \langle d^2(t) \rangle &= MSD(n\Delta t) \\ &= \frac{1}{N-n} \sum_{i=1}^{N-1-n} \left[(x_{i+n} - x_i)^2 + (y_{i+n} - y_i)^2 \right], \end{aligned} \tag{2}$$

where δt corresponds to the time step between two frames.

The increase of the MSD can be quantified by the logarithmic derivative:

$$\beta(t) = \frac{d\ln\langle d^2(t)\rangle}{d\ln(t)}, \quad (3)$$

leading to a time-dependent increase $\langle d^2(t)\rangle = MSD(t) \approx t^{\beta(t)}$.

The persistent random walk equation (24–26) was then used to fit the MSD and determine the different regimes of cell migration:

$$\langle d^2\rangle = 4D_{iff}\left(t - P\left(1 - e^{-t/P}\right)\right). \quad (4)$$

D_{iff} is the diffusion coefficient of the Ornstein-Uhlenbeck (OU) process, and is referred to as the motility coefficient of the cell, and P is the persistence time of the motion.

FA analysis

We first enhanced the contrast by filtering the background and adapting the brightness and contrast. We then used Particle Tracker (ImageJ software) again. We determined the position of the adhesions for each picture, and also the time they appeared and disappeared.

SEM and confocal microscopy

For SEM, we used a previously described procedure (21). We used a confocal microscope (SP5; Leica, Nanterre, France) with a 63× oil immersion objective (HCX APO 63×/1.4-0.60; Leica) and acquired both *Z*- and *Y*-stacks sequentially for different fluorophores.

Immunofluorescent staining

For vinculin and actin fluorescence staining, cells were fixed with 4% paraformaldehyde in PBS for 30 min at room temperature, rinsed three times with PBS, and permeabilized (50 mM of NH_4Cl in PBS for 10 min and 0.1% TritonX-100 in PBS for 4 min). For actin labeling, cells were then stained with either Oregon green-conjugated phalloidin at a dilution of 1:100 or Phalloidin-FluoProbes 547H (Interchim, Montluçon, France) at a dilution of 1:40.

Vinculin staining was performed with the use of a mouse anti-vinculin monoclonal antibody followed by incubation with secondary anti-mouse, fluorescein isothiocyanate-conjugated antibody (Jackson Immuno Research, Suffolk, UK) at a dilution of 1:128.

RESULTS

Micropillar substrate topography

Variable substrates (flat PDMS or micropillar substrates) have been used to compare fibroblast cell behaviors under the same chemical conditions. To promote cell adhesion on these substrates, we coated them with fibronectin. Using confocal microscopy, we verified that fibronectin was uniformly distributed on the pillar fields (see Fig. S1 in the Supporting Material). The dimensions of the pillars and their spacing were chosen to be relevant to modify cell migration processes. To create the substrates, PDMS was molded on etched silicium wafers. The size and shape of the holes, their spacing, and other geometrical parameters were easily varied by the microfabrication process. After PDMS was peeled off from the wafer, the topographical features consisted of a hexagonal array of cylindrical pillars. We varied the height, H, from 2 to 10 μm; the diameter, D, from 5 to 10 μm; and the spacing from edge to edge of the pillars, S, from 5 to 10 μm (see Table S1 and Fig. S2). For clarity, the micropillar substrates will be designated as *H-D-S* in the following. In this study, the pillars were too stiff to be significantly deformed by cells. The spring constants of the pillars under compression, k_n, or shear, k_t, are given by the following formulas:

$$k_n \propto E.\frac{d^2}{L} \text{ and } k_t \propto E.\frac{d^4}{L^3},$$

where E, L, and d are the Young's modulus of the PDMS, and the length and diameter of the pillars, respectively. A rough estimation of the softest pillar spring constants used in this study leads to values of ~8000 and 200 nN/μm for k_n and k_t, respectively.

Cell positioning on the micropillar substrates

After the cells were plated for a few hours (at least 6 h) onto the different micropillar substrates, we used phase-contrast microscopy with low magnification (10×) to observe cell behavior and morphology under various conditions (Fig. 1). Compared with cells on the flat part of the substrates, cells on pillar substrates (6-5-5) appeared to be more branched in shape (Fig. 1 *A*). In addition, the extension of these long protrusions following the grooves appeared to be the key mechanism in guiding cell migration between the micropillar arrays (Fig. 1 *A* and Movie S1). Once they spread on the flat surface, the cells recovered standard 2D shapes with the formation of a large lamellipodium (Movie S1).

On pillars with larger spacing between them (7-10-10), 3T3 cells adopted different morphology and behavior. We observed fewer long and thin extensions than on the (6-5-5) substrates, and pseudopodia-like protrusions that extended on the flat part of the substrate between the pillars (Fig. 1 *B*). The cell body extensions followed the topographical features and anchored around the pillars to move the cell forward (Fig. 1 *B*).

SEM was used to correlate these observations to the positions of the 3T3 cells on micropillar substrates. For a pillar height of ~2 μm, we observed that the morphological responses of the cells due to the topographical features were slightly but not significantly affected by the pillars, and thus were close to those observed on a flat PDMS substrate (Fig. 2 *C*). For the same values of S and D, we observed no major difference in cell positioning and morphology for H of 6–10 μm (Fig. 2).

The adhesion of fibroblast cells strongly depended on the spacing between the pillars. On (6-5-5) substrates, the cell body was mostly localized on the top of pillars, whereas thin extensions that could reach lengths of 50 μm followed the micropillar array and ended in between the pillars (Fig. 2 *A*). Such extensions (i.e., confined by the spacing between the pillars) were not observed on 2D surfaces (Movie S1). By contrast, on (7-10-10) substrates, cells adhered both on top of the pillars and in between them, with the main

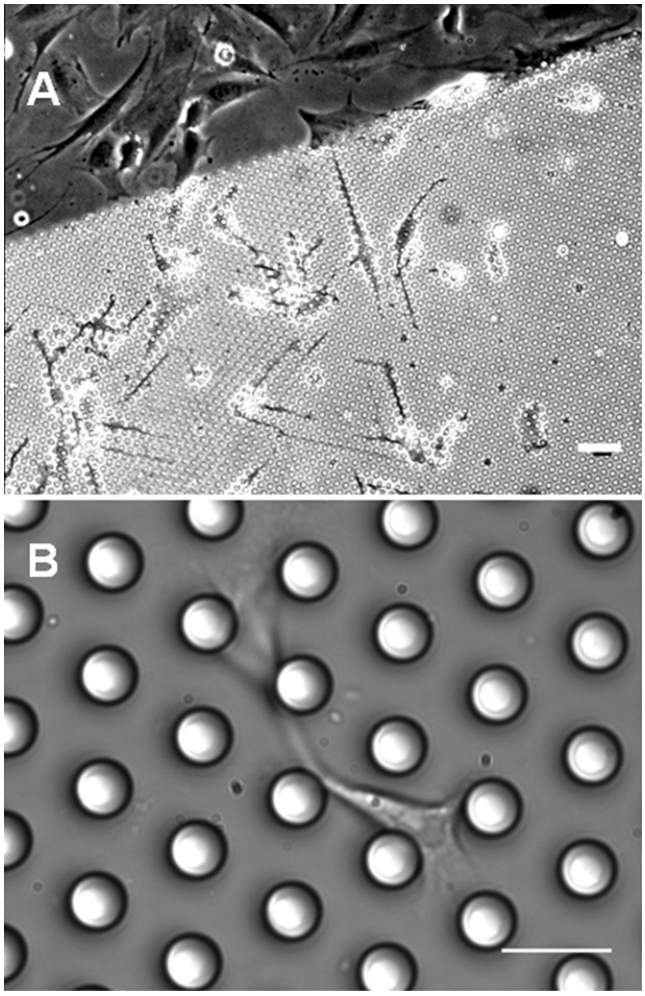

FIGURE 1 Cell adhesion on micropillar substrates. (*A*) Phase-contrast image at the boundary between a flat surface and the micropillar substrate (6-5-5). Scale bar = 50 μm. (*B*) Differential interference contrast image of a cell migrating on a (7-10-10) substrate. Scale bar = 20 μm.

part of the cell body trapped between the pillars. Some of them were thus suspended from pillar to pillar, with anchored extensions guided by the topography and ending on the flat part of the substrate around the pillars (Fig. 2, *B* and *B′*). In both cases, cell body extensions that were constrained by the micropillars dragged cells to move from pillar to pillar. Due to these physical constraints, fibroblasts lacked the well-spread morphology observed in cells moving on 2D substrates. In contrast, a predominantly bi- to tripolar spindle-shaped morphology with matrix-binding pseudopodia in between the pillars, similar to cell shapes in 3D matrices (27), was observed (Fig. 2 *B*).

Morphological responses

We performed a quantitative analysis of the cell morphology by measuring the projected spreading areas of the cells on each substrate and their shape factor. The shape factor was defined as $4\pi A/P^2$, where A is the projected spreading area of the cell, and P is the perimeter. It corresponded to a measure of the degree of branching in cell shape. Concerning the spreading area of the cells, the 3T3 cell surface was sensitive to topographical features since we obtained smaller values of 900 μm^2 on (6-5-5) and (7-10-10) substrates than on a flat PDMS substrate (~2500 μm^2; Fig. 2 *E*). On shorter pillars, the influence of the topography on the spreading of cells was less pronounced (~1700 μm^2 for (2-10-10) and (2-5-5)). For the shape factor, we obtained a value of 0.36 for cells on a flat surface, whereas the (6-5-5) and (7-10-10) substrates gave lower values of 0.25 and 0.22, respectively (Fig. 2 *F*). Again, the values of the shape factor (~0.33 and 0.34 for (2-10-10) and (2-5-5), respectively) on pillars with $H = 2$ μm were found to be closer to the value on the flat surface than those obtained on higher pillars (Fig. 2 *F*). In agreement with our optical microscopy observations, it seemed that the height of the pillars was critical to obtain drastic modifications of the cellular responses as a function of the micropillar substrate. These quantitative data confirmed our SEM and optical microscopy observations, showing a more complex and branched shape of cells on pillar substrates.

Characterization of the migration paths

We performed migration experiments and analyzed the trajectories of migrating 3T3 fibroblasts on flat surfaces and micropillar substrates. The cells were observed for up to 24 h. First, measurements of cell movement indicated that cells on pillar substrates moved at a smaller linear speed, V (Eq. 1), than those on flat regions (15 $\pm$ 7 and 10 $\pm$ 5 μm/h for (6-5-5) and (7-10-10) vs. 23 $\pm$ 10 μm/h, respectively). Since these results showed a large dispersion of speed measurements from one cell to another, we preferred to analyze the MSD displacements over long time periods to determine the effect of topography on cell movements. Fig. 3, *A–C*, depicts the contours and paths of migrating cells for 420 min under three different conditions: flat surface (*A*), (6-5-5) (*B*), and (7-10-10) (*C*). 3T3 cells exhibited more confined trajectories on micropillar substrates than on the flat surface.

At first sight, the trajectories of the cells on the different substrates resembled those of normal Brownian particles. Such a movement should be characterized by an MSD proportional to t^2 at short times corresponding to ballistic motion, and t for long time intervals designating normal diffusion (26). We therefore analyzed the cell motion to determine the characteristics of the trajectories as a function of the topography. In agreement with previous experiments analyzing long-term movements (28), the MSD plotted for the different substrates exhibited a crossover between three different dynamical regimes (Fig. 3 *D*). For short times ($\leq T_1$; phase I), the increase of the MSD did not fit with a ballistic scaling. T_1 values were roughly the same for the different experiments (~20 min). We looked at the logarithmic derivative of the MSD, $\beta(t)$. In this first region, we obtained an exponent β below 1.5. In phase II (up to T_2), the MSD increased with

an exponent whose value depended on the topographical features, varying from 1.3 on a micropillar substrate to 1.45 on a flat one. T_2 appeared as a measurement of the crossover time before a purely diffusive regime. We obtained larger values (~260 and 445 min for (10-5-5) and (10-10-10) substrates, respectively) compared with the one obtained on a flat surface (~130 min). Thus, the duration of the persistent phase increased on micropillar substrates, confirming that the directionality of cell movements was enhanced by topographical features. At larger timescales, the MSD exhibited a transition with an exponent β that gradually decreased to reach values of ~1.0 for the different curves. 3T3 fibroblasts described a diffusive motion at long timescales, in contrast to the one observed for epithelial cells (28).

We confirmed these results by fitting the curves with the persistent random walk equation (Eq. 4), which indicated a good agreement ($R^2 = 0.998$) between our experimental data and the Ornstein–Uhlenbeck (OU) model for $T > T_1$ (Fig. 3). T_1 corresponds to the persistence time, P (Eq. 4). For $T \leq T_1$, since the exponent β was below 1.5, cell movements were not characterized by a ballistic motion as predicted by the OU model. This could explain the differences we observed. However, the statistical significance was not high for short timescales, and further experiments should be performed to confirm the observed behavior. Cell migration over long time periods exhibited a diffusive behavior, as shown by the strong correlation between experimental data and the OU model (Fig. 3 *E*). We analyzed the diffusion coefficients on the different substrates. Fibroblast cells moved less efficiently on micropillar substrates than on a flat surface, resulting in a reduced MSD for all time periods. Moreover, MSDs were also smaller for all time periods on (10-5-5) substrates than on (10-10-10) substrates. Since we obtained a linear relation of the MSD with T for long time intervals for all curves, we measured the diffusion coefficient, D_{iff}, for the different substrates. It was more than twice as large on a flat surface (~11 μm^2/min) as on a (10-10-10) substrate (5 μm^2/min) (Fig. 3 *F*). On a (10-5-5) substrate, the diffusion coefficient

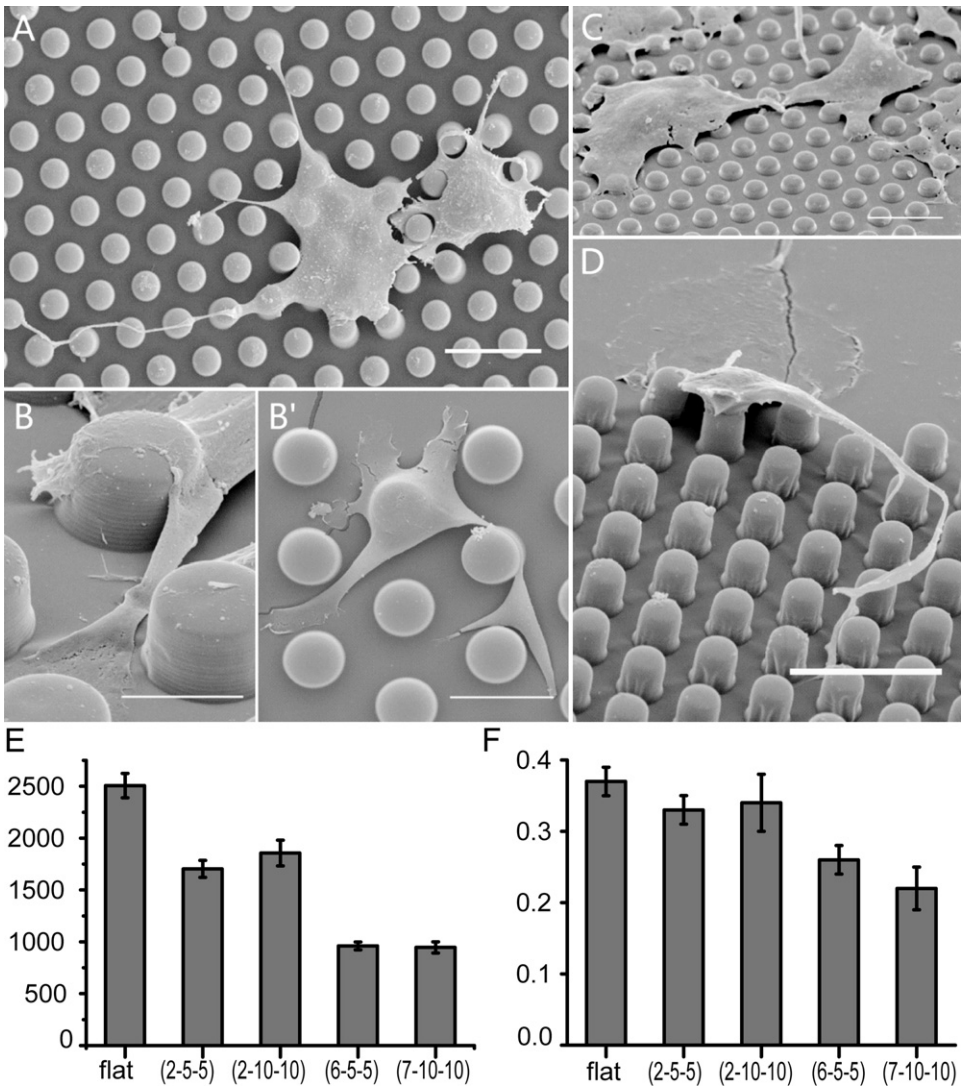

FIGURE 2 SEM pictures of 3T3 cells on the different types of pillars. (*A*) On (10-5-5) substrates, cells are mainly on the top of the pillars and present long protrusions (up to 60 μm). (*B* and *B′*) Cells are spread on the top and in between the pillars, occupying the whole spacing available on the (10-10-10) substrate. (*C*) Spread cells on (2-5-5) substrates present a morphology close to that observed on flat surfaces. (*D*) Cells at the interface between a flat substrate and a (6-5-5) micropillar substrate exhibit a change of morphology, with a large lamellipodium on the flat part and branched structures on the pillars. Scale bars = 20 μm. (*E*) Projected spreading area and (*F*) shape factor of 3T3 cells on flat (2-5-5), (2–10-10), (6-5-5), and (7-10-10) substrates.

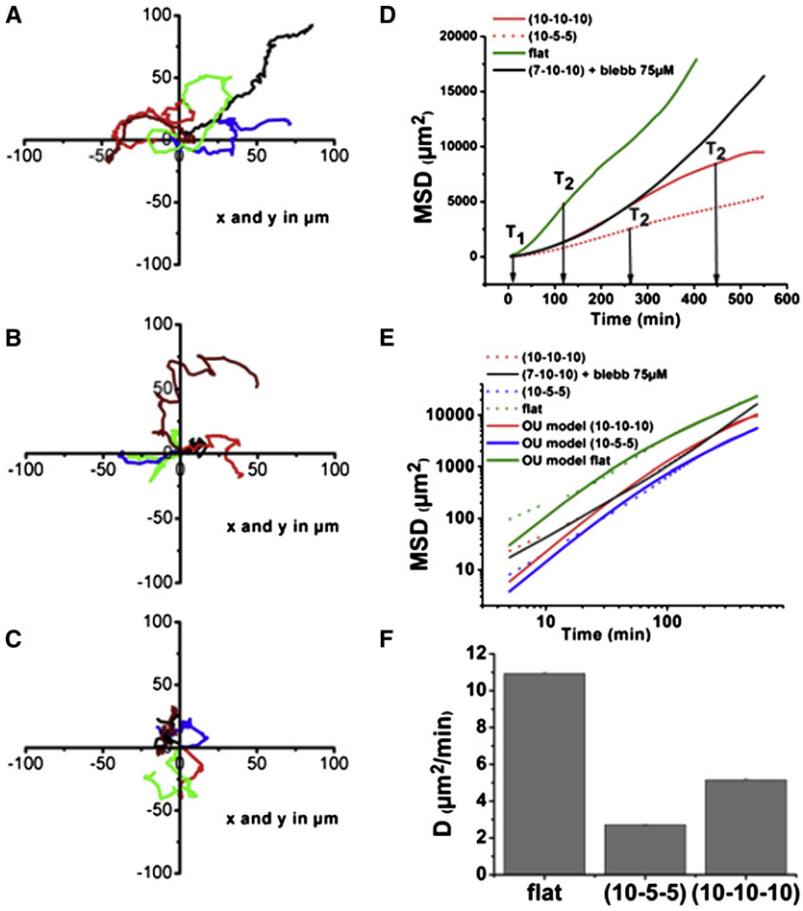

FIGURE 3 Five typical trajectories of 3T3 cells on flat (*A*), (6-5-5) (*B*), and (7-10-10) (*C*) substrates for the same duration (420 min) in the *x-y* plane. (*D*) Plot of the MSD as a function of time for different substrates. T_1 corresponds to the first regime for short timescales. T_2 corresponds to the crossover time before the diffusive regime for a flat substrate and the micropillar substrates ((10-10-10) and (5–10-10)), and is indicated for the different substrates. The black curve represents the MSD of blebbistatin-treated cells. In this case, we do not observe the diffusive regime at long timescales. (*E*) Log-log plots of the MSD as a function of time. Experimental data (*dashed curves*) are fitted by the OU model (*continuous curves*). Each color corresponds to a different substrate. The black curve corresponds to the cells treated with blebbistatin, which cannot be fitted by the OU model because they do not exhibit a diffusive regime. (*F*) Diffusion coefficients, D_{iff}, obtained by the OU model.

was even smaller (2.4 μm^2/min), confirming a cell trapping mechanism at long timescales. On short pillars (H~2 μm), the diffusion coefficients with values of ~6 μm^2/min decreased in comparison with a flat surface but stayed larger than those measured on high-aspect ratio pillars (data not shown).

3T3 cells on micropillar substrates moved less efficiently than 3T3 cells on flat surfaces, showing a reduced MSD for all time periods. Furthermore, cells on (10-10-10) substrates exhibited a smaller MSD than cells on (10-5-5) substrates. The physical constraints of the substrate played a key role in cell movements: the main part of the cell body on (10-5-5) substrates was localized on the top of the pillars, whereas cells on (10-10-10) were completely embedded into the micropillar substrate, with a motility dictated by the spacing and size of the pillars. Thus, a complete analysis of cell trajectories could differentiate among the cell migration mechanisms involved in response to various microenvironments.

Cytoskeleton and FAs organization and dynamics

We hypothesized that the organization of actin cytoskeleton, as well as the formation of FAs (vinculin staining), might differ among the different substrates. We first used confocal microscopy to observe immunofluorescent-stained cells on the micropillars. First, compared with cells spread on a flat substrate (Fig. 4, *A* and *A′*), we observed fewer stress fibers and FAs on micropillar substrates (Fig. 4, *B* and *C′*). On the (7-10-10) substrate, cells were partly spread on the flat area in between the pillars. Actin was mostly recruited around the pillars, but we also observed a strong expression in the formation of arches between two consecutive pillars (Fig. 4 *C* and Movie S2), similar to the one observed on micropatterned 2D surfaces (29). Of interest, cellular branches that were associated with pillars contained actin filaments (see Fig. 4 *C*), confirming that cell movement on pillar substrates was promoted by actin reorganization. The analysis of fluorescently stained cells of vinculin protein showed that these actin-rich structures were colocalized with FAs that were reinforced on the pillar edges, as previously observed (15) (Fig. 4 *C′*). When the average areas of the FAs were measured, they appeared brighter and twice as large on the pillar edges as on the flat part of the substrate (Fig. 5). Larger vinculin structures on pillars indicate that topographic features could increase the formation of FAs (Movie S2 and Fig. 5 *E*). On the (6-5-5) substrates, vinculin-positive structures were mostly distributed on pillars, since a large part of the cell body stayed on the top of the pillars. Again, we observed that thin cellular extensions contained F-actin and that their tips localized on the pillars displayed an important recruitment of vinculin protein (Fig. 4, *B* and *B′*, and Movie S3).

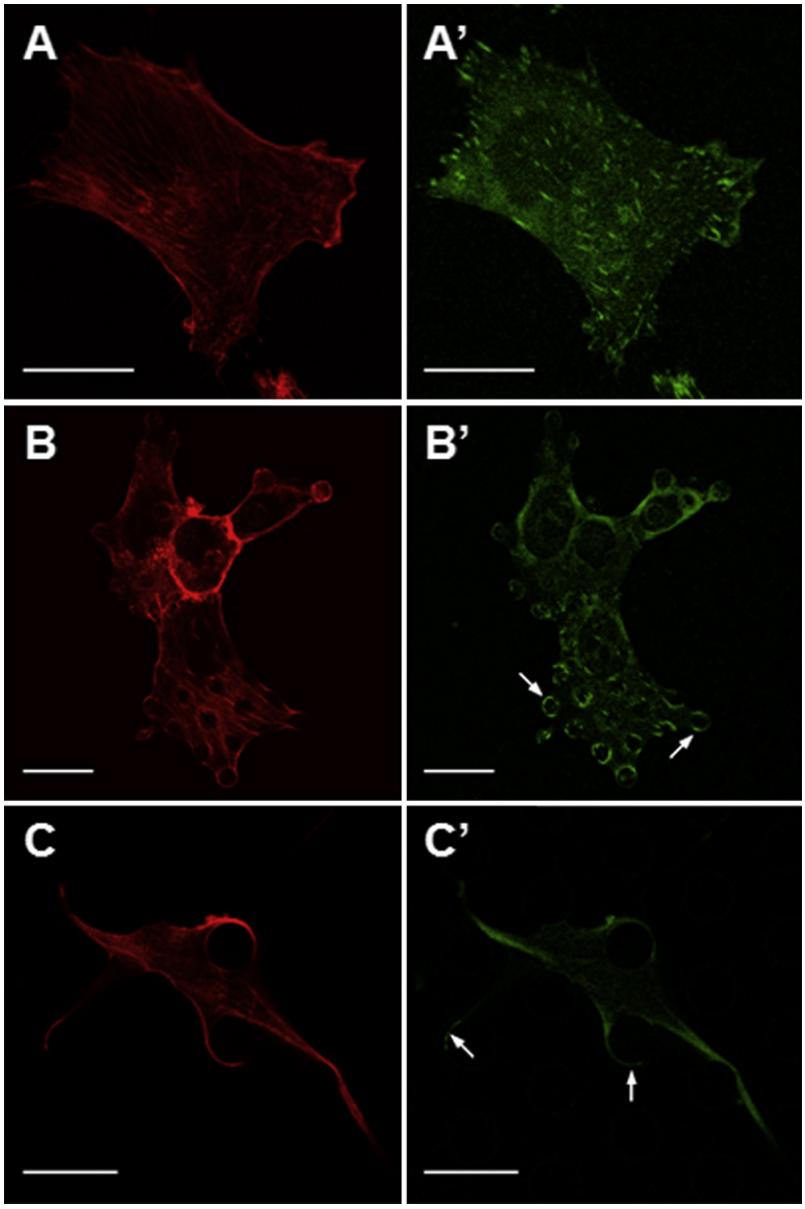

FIGURE 4 Single optical slices of confocal images of immunofluorescent staining of actin (*A–C*) and vinculin (*A′–C′*). (*A* and *A′*) On a flat surface. (*B* and *B′*) On a (6-5-5) substrate. (*C* and *C′*) On (7-10-10) substrates. Fewer stress fibers were observed on the micropillar substrates. FAs are present all over the cell (*A′*), on the top of the pillars, with a diffuse signal in the cytoplasm (*B′*, arrows indicate examples) or only on the side of pillars (*C′*, arrows). Scale bars = 20 μm.

We also compared cells that were located on micropillar substrates and completely spread on a flat PDMS surface (Fig. S3). On fixed samples, vinculin-positive structures presented a dissymmetrical distribution between both parts: the fluorescent cytoplasmic signal was strongly enhanced on the micropillar part, and thus the recruitment of vinculin proteins within FA-like structures was lower on this part of the substrate. Indeed, we observed fewer FAs appearing on the micropillar side (Fig. S3).

Finally, we observed the dynamics of FAs as cells migrated on a micropillar substrate for a 10 μm spacing (7-10-10). We used 3T3 cells expressing EGFP-vinculin to analyze the dynamics of clusters of FA proteins. After seeding overnight, the migration of cells was recorded by time-lapse microscopy over a period of 2 h (Fig. 5). Measuring the turnover of FAs on flat surfaces and pillar substrates allowed us to determine that the lifetime of the FAs was increased when they were formed in the vicinity of the pillars (65 min), in comparison with the flat part of the substrate (18 min; Fig. 5 *F*). Since we used standard fluorescence microscopy to analyze the dynamics of the FAs, the limited *z*-resolution could cause multiple FAs to superimpose on one another, giving rise to an impression of increased stability. However, in most cases, scanning confocal microscopy of fixed cells did not reveal several separated FAs along the same pillar (data not shown). It appeared that the presence of topographical micropillars induced a stabilization of FAs, as previously observed (15). These results confirmed that the previously described cellular protrusions were guided by actin reorganization, and that the topography promoted large and stable clustering of FA proteins.

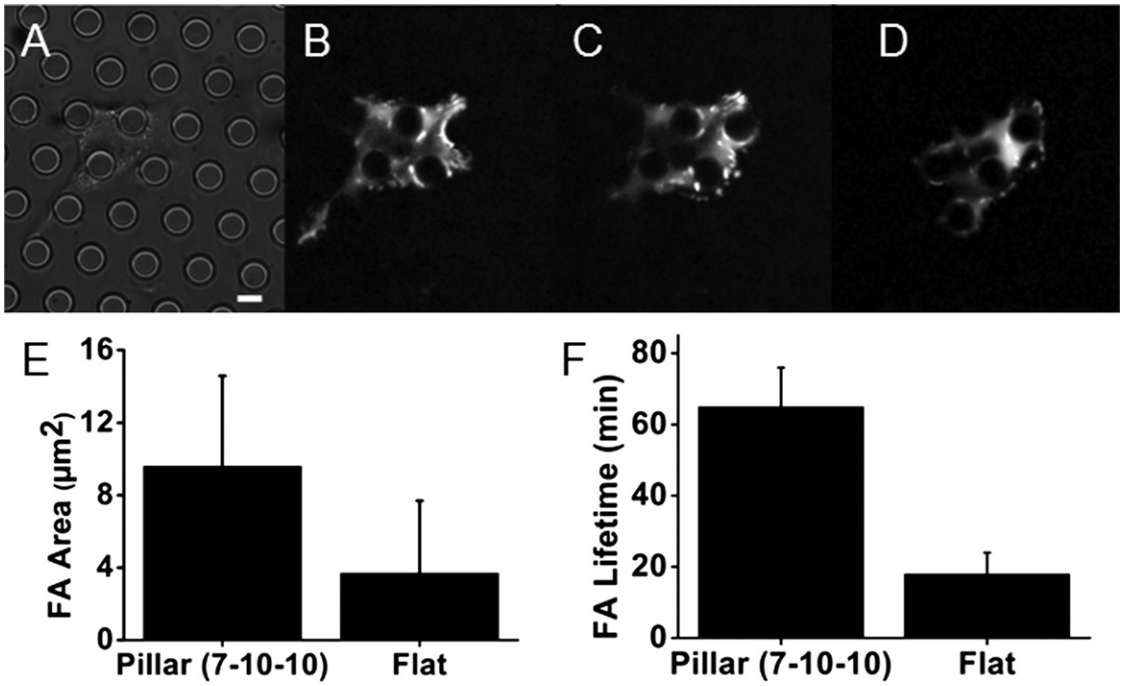

FIGURE 5 Migration of a 3T3 cell stably transfected with EGFP-vinculin plasmid through the micropillar substrate (7-10-10). (*A*) Bright-field image of the micropillars. (*B–D*) Epifluorescent images at different times, *T*, of the distribution of FAs ($T = 0$, 40, and 95 min). Scale bar = 10 μm. (*E*) Stability of FAs (vinculin protein) of 3T3 cells on pillars and flat surfaces between the pillars ((7-10-10) substrate). Bars represent the average lifetime ± SE for ~20 FAs in three cells under each condition. (*F*) Average area of FAs on pillars and flat surfaces between the pillars ((7-10-10) substrate). Bars represent the average area ± SE for ~50 FAs under each condition.

Effects of myosin-driven contractility on cell migration

To investigate the role of the cytoskeleton during cell migration, we modulated actomyosin contractility by perturbing the function of nonmuscle myosin II. First, 3T3 cells were plated onto the micropillar substrates and treated with blebbistatin to inhibit myosin II (30). The blebbistatin-treated cells were even more elongated than the nontreated ones. By analyzing their movement, we found a strongly enhanced directional movement on a (7-10-10) substrate (Fig. 3, *D* and *E*). The MSD of blebbistatin-treated cells followed the same power law for all time periods with an exponent $\beta \sim 1.5$, without any crossover time to a diffusive behavior over 550 min. The removal of contractility prevented the cells from strongly adhering along the micropillars, and thus from changing their migration direction by moving from pillar to pillar.

Cell migration at the frontier between flat and micropillar substrates

We looked at the migration of cells at the frontier between a flat part and a microtextured one to determine if topographical changes of the environment could also induce a preferential direction of cell migration. We focused on two populations of 3T3 cells: one coming from the flat surface, and one coming from the micropillar side of the substrate. We observed cells 6–8 h after plating on the substrates. Their migration was recorded by time-lapse phase microscopy over a period of 12–24 h. For each substrate, observations were successfully made with ~30 cells approaching the boundary from the micropillar side or the flat side. The results reported below were consistently obtained from each set of cells. We observed an influence of topography on cell migration (Fig. 6). On (6-5-5) substrates, 80% of the cells coming from the flat substrate did not cross the boundary ($n = 31$; Fig. 6 *D*). Most of the cells that approached the boundary from the flat side sent some protrusions in between the pillars but stayed on the flat part (Fig. 6 *A* and Movie S4). Some of the cells that still transmigrated stayed between the micropillars, which shows that our observations differ from previous experiments that examined the reactions of cells to single steps on a substratum (31). In contrast, when cells approached the frontier from the micropillar part of the substrate, ~65% of the cells migrated and spread onto the flat substrate (Fig. 6 *E* and Movie S1).

For a larger spacing (10 μm) between the pillars ((7-10-10); Fig. 6, *B* and *E*), a similar result was obtained. We obtained different statistics for cells coming from the flat part for a 10 μm spacing between the pillars; 75% of the cells ($n = 26$) that came to the boundary from the flat substrate migrated through the micropillar (Fig. 6, *C* and *D*). Altogether, these results suggest that the spacing between ''obstacles'' has a role in guiding cell migration. According to these data, a transition occurred for a distance from pillar to pillar of 5–10 μm. The transmigration through micropillar substrates

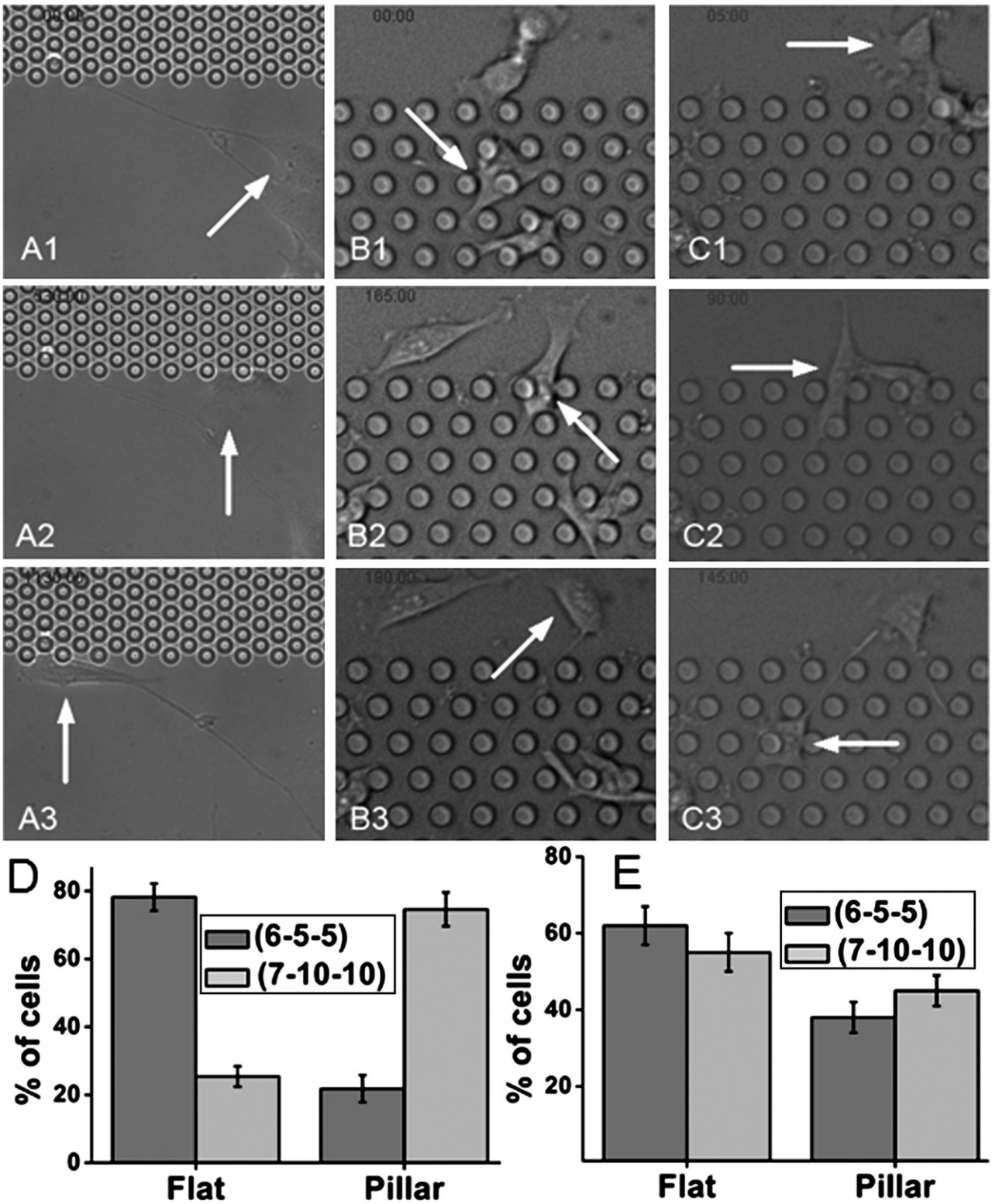

FIGURE 6 Movements of 3T3 cells at the boundary between a micropillar substrate and a flat surface. Images were recorded with phase illumination. (*A*) A cell moved from the flat side of the substrate (6-5-5) toward the micropillar one. The cell moved along the boundary and stayed on the flat side. (*B*) A cell moved from the micropillars on a (6-5-5) substrate toward the flat part of the substrate. The cell migrated through the micropillars and spread on the flat surface. (*C*) A cell moved from the flat side of the substrate (7-10-10) toward the micropillar one. Scale bar = 20 μm; duration ~ 5 h. (*D*) Percentage of cells coming from the flat surface that transmigrate through the micropillar side (Pillar) or stay on the flat side of the substrate (Flat) for two different substrates (6-5-5) and (7-10-10). (*E*) Percentage of cells coming from the micropillar substrate that transmigrate through the flat side (Flat) or stay on the micropillar side of the substrate (Pillar) for two different substrates (6-5-5) and (7-10-10).

was blocked for a 5 μm spacing, whereas most of the cells could transmigrate for a 10 μm one.

DISCUSSION

Cell migration can be random or persistent. In two dimensions, on stiff substrates, cells tend to adopt a polar form with a leading lamellipodium, whereas in three dimensions they can assume elongated or amoeboid morphologies (32). A cell's ability to switch between these migration modes is likely dictated by the way in which it interacts with and responds to the surrounding ECM. Numerous studies have demonstrated that micropatterned substrates can modify cell functions, including adhesion (33,34), migration (15,35,36), and even differentiation (16). However, there have been few systematic analyses of the impact of micro-sized features on cell adhesion and migration mechanisms, even though such substrates could mimic the migration of cells in a 3D matrix with variable porosity.

Here we have shown that substrates with various well-defined geometries affect the adhesion and migration of fibroblasts. Under the same chemical conditions, we varied the geometrical parameters of the substrates (i.e., the diameter, height, and spacing) to analyze the morphology of the cells and the dynamics of cell migration. A major finding of this study is that the degree to which a cell is impeded in its movement is dependent on the size of the features it encounters. Changing the cellular microenvironment switches the cell migration patterns of fibroblasts from a fast and random movement to a slower and persistent movement. By analyzing cell movements on different types of substrates, including a flat surface over long time periods (up to 24 h), we showed that the crossover time between the persistent and the diffusive regimes increased on micropillar substrates. Cells can thus migrate with persistence, allowing their translocation from pillar to pillar. Alternatively, cells on 2D surfaces move rapidly but with lower persistence. Previous studies have demonstrated that this switching mechanism could also be observed in cells moving from 2D to 3D environments, due, for instance, to a lower activity of Rac in 3D cell culture (37). Rac activity promotes the formation of peripheral lamellae, which could mediate random migration. It appeared that decreasing Rac activity as observed in three dimensions suppressed peripheral lamellae and induced a more persistent motion. Although we did not study the activity of Rac, we established that cells presented similar changes in their morphology when plated on bumpy substrates as opposed to flat surfaces. Cells on pillars exhibited a more branched shape than cells on a flat surface, which was similar to cellular shapes observed in 3D environments. We observed that these phenomena strongly depended on the height and spacing between the pillars: very thin and long protrusions were observed for a 5 μm spacing, whereas pseudopodia-like structures were formed in between the pillars for a larger spacing. Such differences highlight the importance of the spacing between the microstructures. The geometrical constraints at the micrometer scale induced morphological changes in the cells by preventing the formation of extended lamellipodia and promoting thin extensions or pseudopodia. Altogether, these results suggest that substrate topography and physical constraints slow down cell movements but increase their persistence. Furthermore, the persistent movement of the cells was enhanced when they adhered mostly on the top of the pillars (6-5-5) instead of migrating in between them (7-10-10). These results can be explained by the formation of specific cellular protrusions on micropillar substrates—either thin and long cell extensions or pseudopods, depending on the spacing between the pillars. We hypothesized that such protrusions could help to guide the directionality of cell movements.

We next examined the organization of actin and FAs to explain the reduced MSD and the increased persistent motion observed on pillars. Our immunofluorescent-staining experiments indicated the presence of F-actin in the cellular protrusions that extended from pillar to pillar. However, we observed fewer stress fibers and FAs on micropillar substrates as compared with flat surfaces. Since an important part of the cell body was localized on the top of the pillars for a 5 μm spacing, we observed FAs on pillars. For a 10 μm spacing, FAs were formed both on flat surfaces and on the pillars. However, they appeared larger and more stable over time on the pillars. Thus, it appears that the micropillars promote the guidance of actin cables and the formation of FAs, as previously shown on various substrates (15,38). The contractile cell machinery plays a key role in governing cell movements in response to topography. The formation of strong actin cables from pillar to pillar on both 5 and 10 μm spacings could thus explain why the cell movements showed longer persistence on micropillars than on flat surfaces. In addition, this assumption was confirmed by the presence of FAs on the top of pillars for a 5 μm spacing, and their increased length and stability over time on pillars with a 10 μm spacing. Since FAs are known to regulate traction forces (11), their preferential location at pillars drive the directionality of cell migration and induce a longer persistent movement than on a flat surface. In other words, a possible mechanism for cell movements on micropillar substrates could be that the topography enhances the formation of adhesive contacts in the vicinity of the pillars and thus promotes cell migration from pillar to pillar, leading to motions directed by the geometrical constraints (Fig. S4 *A*). In particular, when the main part of the cell body is localized between the pillars (10 μm spacing), the formation of pseudopods between the pillars that frequently end up adhering along neighboring pillars can serve to pull the cell body forward. The increased FA lifetimes along the pillars ((7-10-10); Fig. 5 *E*) can also partly explain the slower dynamics of cell movements obtained on micropillar substrates as compared with flat surfaces.

The cellular response to substrate topography shows similarities to the responses to substrate rigidity. Previous studies

have shown that fibroblasts exert stronger traction forces on stiff substrates than on soft ones (8,34), which is correlated with an enhancement of anchorage through FAs. One can hypothesize that the substrate micropattern may increase the density of local contacts through integrin clustering. The contractility, when the cell is anchored to the pillars through the FAs, allows the cell to move forward by sensing the topography. This result was confirmed by the experiments with blebbistatin-treated cells. Previous studies have shown that myosin II contractility was required for cell shape regulation (15,39). Here, the inhibition of nonmuscle myosin II induced persistent cell motion over long timescales, as if the geometrical constraints imposed by the micropillar hexagonal array were the only important parameter that restricted cell movements (Fig. S4 *B*).

Finally, our experiments performed at the frontier between the bumpy surface and the flat one confirmed that the ability of cells coming from the flat surface to cross this frontier was compromised or enhanced for a 5 or 10 μm spacing, respectively. Again, the cells' ability to preferentially migrate through the micropillar substrate for a 10 μm spacing could be explained by a enhanced stability of FAs along the pillars, which could provide enough traction forces for transmigration. In addition, our experiments indicate a critical distance between these two values for the transmigration of fibroblasts through microenvironments. For now, the exact interpretation of this critical distance is still unclear. However, we can assume that the nucleus, and especially its stiffness (40), could play a key role in the migration on micropillar substrates by probing the topographical features to be deformed. Further experiments should clarify this point.

In this work we performed an extensive study of cell responses to substrate topography. Our results show that both cellular and molecular functions are affected by the geometrical features of the substrate. Understanding these different behaviors may be useful for developing strategies to discriminate between cellular phenotypes.

SUPPORTING MATERIAL

One table, four figures, and four movies are available at http://www.biophysj.org/biophysj/supplemental/S0006-3495(09)00854-6.

We thank A. Buguin, K. Dahl, G. Grégoire, J.-M. di Meglio, P. Silberzan, and Y.-L. Wang for helpful discussions. The SEM was performed with the help of D. Montero at the Centre Interuniversitaire de Microscopie Electronique (Paris). Confocal acquisitions were performed at the Imaging Platform at the Institut Jacques Monod (Paris). This work was performed in part at the Institut d'Electronique, de Microélectronique, de Nanotechnologie Laboratory (Villeneuve d'Ascq, France).

L.T. received postdoctoral grants from the Agence Nationale de la Recherche (ANR). This work was partly supported by grants from the ANR (Program PNANO 2005), the region Ile-de-France (C'Nano Program), the Centre National de la Recherche Scientifique (Programme Prise de Risque 2008), the Association Française contre les Myopathies, and the Ligue Contre le Cancer.

REFERENCES

1. Comoglio, P. M., and L. Trusolino. 2005. Cancer: the matrix is now in control. *Nat. Med.* 11:1156–1159.
2. Lauffenburger, D. A., and A. F. Horwitz. 1996. Cell migration: a physically integrated molecular process. *Cell.* 84:359–369.
3. Even-Ram, S., and K. M. Yamada. 2005. Cell migration in 3D matrix. *Curr. Opin. Cell Biol.* 17:524–532.
4. Cukierman, E., R. Pankov, and K. M. Yamada. 2002. Cell interactions with three-dimensional matrices. *Curr. Opin. Cell Biol.* 14:633–639.
5. Kuntz, R. M., and W. M. Saltzman. 1997. Neutrophil motility in extracellular matrix gels: mesh size and adhesion affect speed of migration. *Biophys. J.* 72:1472–1480.
6. Vogel, V., and M. Sheetz. 2006. Local force and geometry sensing regulate cell functions. *Nat. Rev. Mol. Cell Biol.* 7:265–275.
7. Discher, D. E., P. Janmey, and Y. L. Wang. 2005. Tissue cells feel and respond to the stiffness of their substrate. *Science.* 310:1139–1143.
8. Lo, C. M., H. B. Wang, M. Dembo, and Y. L. Wang. 2000. Cell movement is guided by the rigidity of the substrate. *Biophys. J.* 79:144–152.
9. Saez, A., M. Ghibaudo, A. Buguin, P. Silberzan, and B. Ladoux. 2007. Rigidity-driven growth and migration of epithelial cells on microstructured anisotropic substrates. *Proc. Natl. Acad. Sci. USA.* 104:8281–8286.
10. Giannone, G., B. J. Dubin-Thaler, H. G. Dobereiner, N. Kieffer, A. R. Bresnick, et al. 2004. Periodic lamellipodial contractions correlate with rearward actin waves. *Cell.* 116:431–443.
11. Riveline, D., E. Zamir, N. Q. Balaban, U. S. Schwarz, T. Ishizaki, et al. 2001. Focal contacts as mechanosensors: externally applied local mechanical force induces growth of focal contacts by an mDia1-dependent and ROCK-independent mechanism. *J. Cell Biol.* 153: 1175–1185.
12. Tzvetkova-Chevolleau, T., A. Stephanou, D. Fuard, J. Ohayon, P. Schiavone, et al. 2008. The motility of normal and cancer cells in response to the combined influence of the substrate rigidity and anisotropic microstructure. *Biomaterials.* 29:1541–1551.
13. Curtis, A., and C. Wilkinson. 1997. Topographical control of cells. *Biomaterials.* 18:1573–1583.
14. Kaiser, J. P., A. Reinmann, and A. Bruinink. 2006. The effect of topographic characteristics on cell migration velocity. *Biomaterials.* 27:5230–5241.
15. Frey, M. T., I. Y. Tsai, T. P. Russell, S. K. Hanks, and Y. L. Wang. 2006. Cellular responses to substrate topography: role of myosin II and focal adhesion kinase. *Biophys. J.* 90:3774–3782.
16. Steinberg, T., S. Schulz, J. P. Spatz, N. Grabe, E. Mussig, et al. 2007. Early keratinocyte differentiation on micropillar interfaces. *Nano Lett.* 7:287–294.
17. Berry, C. C., G. Campbell, A. Spadiccino, M. Robertson, and A. S. G. Curtis. 2004. The influence of microscale topography on fibroblast attachment and motility. *Biomaterials.* 25:5781–5788.
18. Mandeville, J. T. H., M. A. Lawson, and F. R. Maxfield. 1997. Dynamic imaging of neutrophil migration in three dimensions: mechanical interactions between cells and matrix. *J. Leukoc. Biol.* 61:188–200.
19. Zaman, M. H., L. M. Trapani, A. Siemeski, D. MacKellar, H. Y. Gong, et al. 2006. Migration of tumor cells in 3D matrices is governed by matrix stiffness along with cell-matrix adhesion and proteolysis. *Proc. Natl. Acad. Sci. USA.* 103:10889–10894.
20. Hollister, S. J., R. D. Maddox, and J. M. Taboas. 2002. Optimal design and fabrication of scaffolds to mimic tissue properties and satisfy biological constraints. *Biomaterials.* 23:4095–4103.
21. du Roure, O., A. Saez, A. Buguin, R. H. Austin, P. Chavrier, et al. 2005. Force mapping in epithelial cell migration. *Proc. Natl. Acad. Sci. USA.* 102:2390–2395.

22. Rabodzey, A., P. Alcaide, F. W. Luscinskas, and B. Ladoux. 2008. Mechanical forces induced by the transendothelial migration of human neutrophils. *Biophys. J.* 95:1428–1438.

23. Sbalzarini, I. F., and P. Koumoutsakos. 2005. Feature point tracking and trajectory analysis for video imaging in cell biology. *J. Struct. Biol.* 151:182–195.

24. Shreiber, D. I., V. H. Barocas, and R. T. Tranquillo. 2003. Temporal variations in cell migration and traction during fibroblast-mediated gel compaction. *Biophys. J.* 84:4102–4114.

25. Selmeczi, D., S. Mosler, P. H. Hagedorn, N. B. Larsen, and H. Flyvbjerg. 2005. Cell motility as persistent random motion: theories from experiments. *Biophys. J.* 89:912–931.

26. Uhlenbeck, G. E., and L. S. Ornstein. 1930. On the theory of the Brownian motion. *Phys. Rev.* 36:0823–0841.

27. Friedl, P., and E. B. Brocker. 2000. The biology of cell locomotion within three-dimensional extracellular matrix. *Cell. Mol. Life Sci.* 57:41–64.

28. Dieterich, P., R. Klages, R. Preuss, and A. Schwab. 2008. Anomalous dynamics of cell migration. *Proc. Natl. Acad. Sci. USA.* 105:459–463.

29. Thery, M., V. Racine, M. Piel, A. Pepin, A. Dimitrov, et al. 2006. Anisotropy of cell adhesive microenvironment governs cell internal organization and orientation of polarity. *Proc. Natl. Acad. Sci. USA.* 103:19771–19776.

30. Limouze, J., A. F. Straight, T. Mitchison, and J. E. Sellers. 2004. Specificity of blebbistatin, an inhibitor of myosin II. *J. Muscle Res. Cell Motil.* 25:337–341.

31. Clark, P., P. Connolly, A. S. G. Curtis, J. A. T. Dow, and C. D. W. Wilkinson. 1987. Topographical control of cell behavior. 1. Simple step cues. *Development.* 99:439–448.

32. Sahai, E. 2005. Mechanisms of cancer cell invasion. *Curr. Opin. Genet. Dev.* 15:87–96.

33. Chen, C. S., M. Mrksich, S. Huang, G. M. Whitesides, and D. E. Ingber. 1997. Geometric control of cell life and death. *Science.* 276:1425–1428.

34. Ghibaudo, M., A. Saez, L. Trichet, A. Xayaphoummine, J. Browaeys, et al. 2008. Traction forces and rigidity sensing regulate cell functions. *Soft Matter.* 4:1836–1843.

35. Jiang, X. Y., D. A. Bruzewicz, A. P. Wong, M. Piel, and G. M. Whitesides. 2005. Directing cell migration with asymmetric micropatterns. *Proc. Natl. Acad. Sci. USA.* 102:975–978.

36. Gustavsson, P., F. Johansson, M. Kanje, L. Wallman, and C. E. Linsmeier. 2007. Neurite guidance on protein micropatterns generated by a piezoelectric microdispenser. *Biomaterials.* 28:1141–1151.

37. Pankov, R., Y. Endo, S. Even-Ram, M. Araki, K. Clark, et al. 2005. A Rac switch regulates random versus directionally persistent cell migration. *J. Cell Biol.* 170:793–802.

38. Walboomers, X. F., W. Monaghan, A. S. G. Curtis, and J. A. Jansen. 1999. Attachment of fibroblasts on smooth and microgrooved polystyrene. *J. Biomed. Mater. Res.* 46:212–220.

39. Mader, C. C., E. H. Hinchcliffe, and Y. L. Wang. 2007. Probing cell shape regulation with patterned substratum: requirement of myosin II-mediated contractility. *Soft Matter.* 3:357–363.

40. Dahl, K. N., P. Scaffidi, M. F. Islam, A. G. Yodh, K. L. Wilson, et al. 2006. Distinct structural and mechanical properties of the nuclear lamina in Hutchinson-Gilford progeria syndrome. *Proc. Natl. Acad. Sci. USA.* 103:10271–10276.